

## THE INFLUENCE OF CORRUGATED PIPES PARAMETERS ON HEAT TRANSFER CHARACTERISTICS

by

**Hongzhe ZHAI<sup>a</sup>, Sasa GAO<sup>a\*</sup>, Wenjie ZHANG<sup>a</sup>, Yuan SONG<sup>b,c\*</sup>,  
Xuepeng GONG<sup>b,c</sup>, Dazhuang WANG<sup>b,c</sup>, and Qipeng LU<sup>b,c</sup>**

<sup>a</sup> School of Mechanical and Electrical Engineering,  
Shaanxi University of Science and Technology, Xi'an, China

<sup>b</sup> Key Laboratory of Optical System Advanced Manufacturing Technology,  
Chinese Academy of Sciences, Changchun, China

<sup>c</sup> State Key Laboratory of Applied Optics, Chinese Academy of Sciences, Changchun, China

Original scientific paper

<https://doi.org/10.2298/TSCI230709231Z>

*In order to investigate the influence mechanism of various corrugated structures on the heat transfer of continuous annular concave-convex corrugated pipes, this paper examines the influence of corrugation height ( $C_h = 1\text{ mm}$ ,  $1.5\text{ mm}$ , and  $2\text{ mm}$ ) and corrugation width ( $C_w = 1\text{ mm}$ ,  $1.5\text{ mm}$ , and  $2\text{ mm}$ ) on the flow pattern, turbulent kinetic energy, Nusselt number, friction coefficient, and performance evaluation factor. Then, the correlation equations for Nusselt number and friction coefficient are established with different corrugated structural parameters. The results show that with the increase of  $C_h$ , the vortex number, turbulent kinetic energy, and friction coefficient in the pipe increase while Nusselt number decreases. The maximum performance evaluation factor is 0.90 at  $C_h = 1\text{ mm}$ . However, with the increase of  $C_w$ , the vortex number and Nusselt number in the pipe increase, while turbulent kinetic energy and friction coefficient in the pipe do not change much. The maximum performance evaluation factor is 0.87 at  $C_w = 2\text{ mm}$ . Therefore, for this type of corrugated pipe, one should choose a small  $C_h$  and a large  $C_w$ .*

*Key words: corrugated pipes, heat transfer, enhanced heat transfer, numerical simulation*

### Introduction

The continuous annular concave-convex corrugated pipes are heat transfer mediums with self-cleaning functions, widely used in heat recovery, waste heat utilization, medical treatment, scientific research, and other fields [1-3]. For example, the heat transfer performance of the cooling tube used in the Synchrotron Radiation double crystal monochromator directly affects the stability of the light emitted [3]. Since the influence mechanism of corrugation-related structural parameters on the heat transfer of corrugated pipes has yet to be specified, it is urgent to optimize its structural parameters to improve the cooling system's heat transfer performance and structural stability.

In the current research, the active heat transfer enhancement technology generally relies on the external stirring and vibration. In contrast, passive heat transfer enhancement technology mainly increases the heat transfer coefficient by changing the structural configuration to enhance heat transfer [4, 5]. Laohalertdecha and Somchai [6] and Ma *et al.* [7] studied the flow, heat transfer, and pressure drop in smooth and corrugated pipes with different refrigerants by changing the

\* Corresponding author, e-mail: [gaosasa@sust.edu.cn](mailto:gaosasa@sust.edu.cn); [songyuan\\_show@126.com](mailto:songyuan_show@126.com)

corrugation pitch and gap number. The results show that the average heat transfer coefficient and pressure drop increase with mass flux and average mass increase. Increasing the number of corrugation gaps can improve friction loss and heat transfer performance more than increasing the number of corrugation pitches. Kown *et al.* [8], Jiang *et al.* [9], and Jaffal *et al.* [10] found that corrugated pipes show significantly better heat transfer performance with larger corrugation angles, higher corrugation heights, and spacing ratio at the Reynolds numbers, between 200 and 1200. Al-Obaidi and Alhamid [11], Al-Obaidi [12], and Al-Obaidi and Alhamid [13] conducted a numerical study to investigate the heat transfer performance of eight corrugated pipes with discontinuous and tiny corrugated structures. It was found that the heat transfer performance of the corrugated pipe increased with decreasing the distance between arc ring, corrugated arc ring angle, and distance between the corrugated ring, while the arc ring angle around the pipe, corrugated pipe ratio, number of the corrugated rings, corrugated diameter ring, and corrugated ring diameter showed the opposite trend. Han *et al.* [14] and Ajeel *et al.* [15] investigated the effect of four special-shaped corrugated structures on the heat transfer performance of corrugated pipes. The results show that the heat transfer performance of symmetrical corrugated pipes is higher than that of asymmetrical corrugated pipes and that optimizing the groove radius and groove profile can maximize the heat transfer performance.

Several researchers [16-21] investigated the heat transfer performance of spiral corrugated pipes with different parameters under constant heat flow and different Reynolds number. The results show that users can choose a high-roughened corrugated pipe when Reynolds number is low ( $Re \leq 4000$ ). When Reynolds number is high ( $4000 < Re < 12000$ ), it is the opposite. Increasing the concave degree of the pipe wall and the corrugation inclination angle, changing the depth ratio of the thread, and reducing the pitch ratio can increase heat transfer performance. Qi *et al.* [22] studied the heat and mass transfer flow characteristics of  $TiO_2$ -water nanofluids in stainless steel corrugated pipes and smooth pipes through experiments and numerical methods. It shows that the combination of corrugated pipes and  $TiO_2$ -water nanofluid exhibits excellent heat transfer performance, and the Nusselt number increases with the increase of Reynolds number, while the friction coefficient,  $f$ , is gradually decreasing. Some scholars [23-25] combined active and passive heat transfer enhancement techniques to study nanofluids' flow and heat transfer characteristics in different corrugated pipes and smooth pipes. Although the heat transfer performance has been significantly improved, the long-term use of active heat transfer enhancement techniques will cause waste. Changing the corrugation's rib shape and pitch ratio of the spiral corrugation can improve the heat transfer performance of corrugated pipes by destroying the temperature boundary-layer.

Researchers have extensively investigated heat and mass transfer enhancement mechanisms and structural parameters of corrugated pipe heat exchangers with tiny, discontinuous corrugated features [11-16, 23-25]. However, the heat transfer mechanism of continuous annular concave-convex corrugated pipes with large corrugation size configurations still needs to be clarified. Therefore, this research aims to establish a numerical analysis model to improve its heat transfer characteristics in the range of  $Re = 4000-12000$  by changing the corrugation height,  $C_h$ , and corrugation width,  $C_w$ , of the continuous annular concave-convex corrugated pipes. Then, the correlation equations for Nusselt number and  $f$  are established with different corrugated structural parameters.

## Corrugated pipe physical model description and boundary conditions

### Physical pipes models descriptions

Figure 1 shows the physical model of the corrugated pipe. The length of the pipe is  $L = 300$  mm, and the equivalent diameter of the corrugated pipe is  $D_h = 10$  mm. The parameters

of the corrugated cooling tube used in the double crystal monochromator in SSRF are  $C_h \approx 1.2$  mm and  $C_w \approx 1.5$  mm [26]. However, the influence mechanism of the structural parameters of corrugated pipe on its heat transfer performance has not been specified. In order to specify this problem, the corrugation structures with  $C_h = 1$  mm, 1.5 mm, and 2 mm and  $C_w = 1$  mm, 1.5 mm, and 2 mm are chosen. In order to ensure that the fluid entering the corrugated pipes stage develops well into a turbulent flow, the length of the inlet smooth pipe is  $L_i = 100$  mm, and that of the corrugated section is  $L_c = 180$  mm, while the outlet length is  $L_o = 20$  mm, in order to prevent the fluid backflow. It's assumed that the heat exchange only exists in the corrugated section.

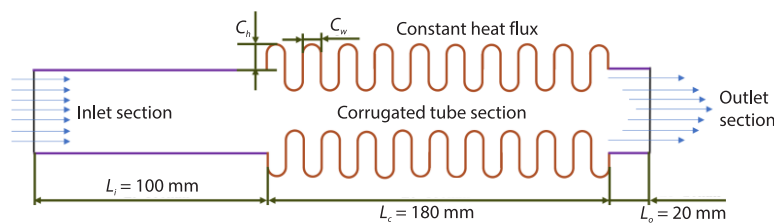


Figure 1. Physical model of corrugated pipe

### Boundary conditions

In this numerical calculation, the working fluid is water, Reynolds number is controlled between 4000-12000, and the inlet water temperature is  $T_i = 293$  K. A constant heat flux ( $\Phi_q = 796$  W/m<sup>2</sup>) is applied on the corrugated section [11-13, 22], while the boundary conditions are velocity inlet and pressure outlet. Zero static pressure is maintained at the inlet and outlet, and a no-slip boundary condition is applied on the pipe wall. Table 1 shows the water's relevant physical parameters and the relevant boundary conditions of the simulation.

Table 1. The parameters of working fluid and boundary conditions

Properties	H <sub>2</sub> O	Boundary conditions	
Density [kgm <sup>-3</sup> ]	998.2	Inlet velocity 1 [ms <sup>-1</sup> ]	0.419
$C_p$ [Jkg <sup>-1</sup> K <sup>-1</sup> ]	4182	Inlet velocity 2 [ms <sup>-1</sup> ]	0.603
Thermal conductivity [Wm <sup>-1</sup> K <sup>-1</sup> ]	0.6	Inlet velocity 3 [ms <sup>-1</sup> ]	0.804
Viscosity [kgm <sup>-1</sup> s <sup>-1</sup> ]	0.001003	Inlet velocity 4 [ms <sup>-1</sup> ]	1.005
Molecular weight [-]	18.0152	Inlet velocity 5 [ms <sup>-1</sup> ]	1.206
Standard state enthalpy [kJmol <sup>-1</sup> ]	285.830	Constant heat flux [Wm <sup>-2</sup> ]	796

### Numerical calculation model

#### Computational analysis model

This numerical analysis calculation was executed with the steady-state solver in FLU-ENT software, using the RNG  $k$ - $\epsilon$  turbulence model [11-13]. The convergence scales of the continuity, momentum, and turbulence equations are all at the magnitude of  $10^{-6}$ , while the convergence scale of the energy equation is at the magnitude of  $10^{-7}$ . Turbulent kinetic energy (TKE) and energy second-order upwind discrete equations are adopted. The relevant control equations can be seen in references [12, 13], which will not be detailed here.

### Mesh generation and independence test

HyperMesh software is used to divide the asymmetrically structured mesh, as shown in fig. 2. It's necessary to conduct boundary-layer meshing at the walls to ensure the calculation accuracy.

Figure 3 shows the comparative analysis of the mesh independence verification of corrugated pipes meshes with mesh numbers of  $3.3 \times 10^6$ ,  $4.4 \times 10^6$ ,  $5.5 \times 10^6$ ,  $6.6 \times 10^6$ ,  $7.7 \times 10^6$ ,  $8.8 \times 10^6$ , and keeping the  $Y^+$  value of the wall less than 1. The objects of the verification  $f$  and Nusselt number. When the mesh number reaches to  $7.7 \times 10^6$ , the mesh can be considered independent, while the errors of  $f$  and Nusselt number are 1.612 % and 0.282 %, respectively.

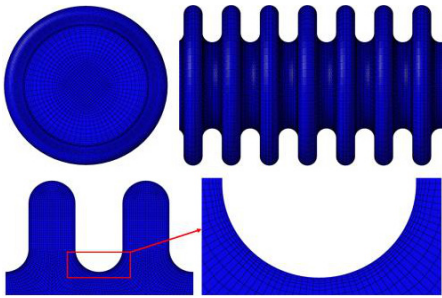


Figure 2. Mesh model of corrugated pipe

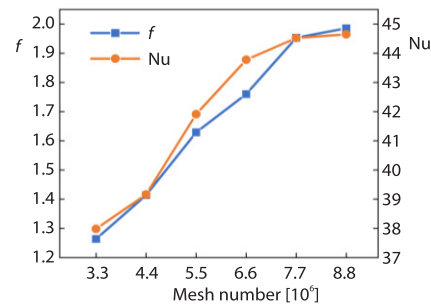


Figure 3. Mesh independence verification

### Data reduction

The Reynolds number is a dimensionless number that can be used to characterize fluid-flow conditions, which can be expressed [27]:

$$\text{Re} = \frac{\rho D_h u}{\mu} \quad (1)$$

The heat transfer coefficient is defined:

$$h = \frac{\Phi}{A(T_{\text{wall}} - T_{\text{ref}})} \quad (2)$$

where  $\Phi$ ,  $A$ ,  $T_{\text{wall}}$ , and  $T_{\text{ref}}$  are the total heat rate, heating area, local wall temperature of the wall at the corrugation, and the overall temperature at the corrugation, respectively.

The local Nusselt number and  $f$  can be expressed:

$$\text{Nu} = \frac{h D_h}{\lambda} \quad (3)$$

$$f = \frac{2 D_h \Delta P}{\rho u^2 \Delta L} \quad (4)$$

where  $\lambda$  is the thermal conductivity of the fluid and  $\Delta P/\Delta L$  – the pressure drop per unit length.

The performance evaluation factor (PEF) is a significant parameter [27]:

$$\text{PEF} = \frac{\text{Nu}}{\text{Nu}_0} \left( \frac{f}{f_0} \right)^{1/3} \quad (5)$$

where  $f_0$  and  $\text{Nu}_0$  are the smooth pipe's friction coefficient and Nusselt number.

### Numerical validation

In order to verify the accuracy of the numerical analysis, Nusselt number and  $f$  of the corrugated pipes were compared with that of the experimental data from  $Q_i$  [22], measured at Reynolds number between 4000-12000. The numerical results in this research show good agreement with the experimental data of  $Q_i$ , which can be seen in fig. 4. The maximum deviation of Nusselt number is 4.5%, mainly occurring at  $Re = 5600$ , while the maximum deviation of  $f$  occurs at  $Re = 7000$  with the value of 5.6 %.

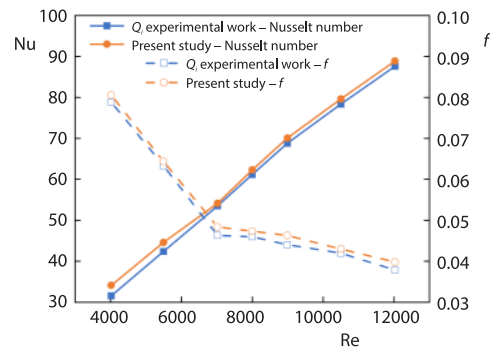


Figure 4. Numerical validation

### Results and discussion

This section studies the effects of different corrugated structures parameters on the heat transfer of corrugated pipes, and the flow in the pipe, TKE, Nusselt number,  $f$ , and PEF are discussed completely. Firstly, the effect of  $C_h$  on heat transfer of corrugated pipes is investigated,  $C_w$  is fixed at 1.5 mm according to the size of the corrugated pipes used in Synchrotron Radiation [27]. Then, according to the parameter control method,  $C_h$  is fixed at 1.5 mm while studying the influence of  $C_w$  on the heat transfer performance of the corrugated pipes. Finally, the correlation equations for Nusselt number and  $f$  are established.

#### Effect of corrugation height

Figure 5 shows the CFD results of the pipe-line's velocity distributions and streamlines. With the increase of  $C_h$ , the velocity of the main flow area in the pipe-line will also increase. The flow velocity in the main flow area increases with the increase of pressure drop per unit length. The vortex will form inside the corrugated ring with different  $C_h$ , and a little secondary flow will form at the transition connection of the concave and convex corrugations. The continuous concave and convex corrugations inside the pipe change the flow direction from axial flow to radial flow. Thus, the size and number of vortices also show differences with the increment of  $C_h$ , which can be seen in fig. 5. When  $C_w$  is determined, the larger  $C_h$ , there will be more vortices. These vortices and the secondary flow are also essential to improve the heat transfer characteristics of the corrugated pipes.

The TKE contour distribution map is shown in fig. 6 when  $C_h$  is 1 mm, 1.5 mm, and 2 mm, respectively. It can be observed that in the flow process of fluid, TKE in the pipe increases with the increase of  $C_h$ . The TKE at the corrugated connections is more significant than that in the main flow area, which means that the liquid between the corrugated ring area and the main flow area is more likely to produce circular flow and liquid mixing. Due to the liquid-flow direction, TKE near the right side of the corrugation is more significant than that on the left side. The impact of the liquid on the wall causes a vortex, resulting in a larger TKE. This phenomenon also disrupts the thermal boundary-layer, increasing the value of  $f$  and Nusselt number of fluid-flow in the pipe. When  $C_h$  is 2 mm, the maximum value of TKE is about 0.44 J/kg.

Figure 7(a) compares the local Nusselt number of the corrugated pipe and the smooth pipe when  $C_h$  is 1 mm, 1.5 mm, and 2 mm. It can be seen that Nusselt number increases as Reynolds number increases. At the same time, the local Nusselt number increases as  $C_h$  decreases. When  $C_h$  is 2 mm, Reynolds number is in the range of 4000-10000, Nusselt number is lower than that of the smooth pipe, while Reynolds is in the range of 10000-12000, Nusselt

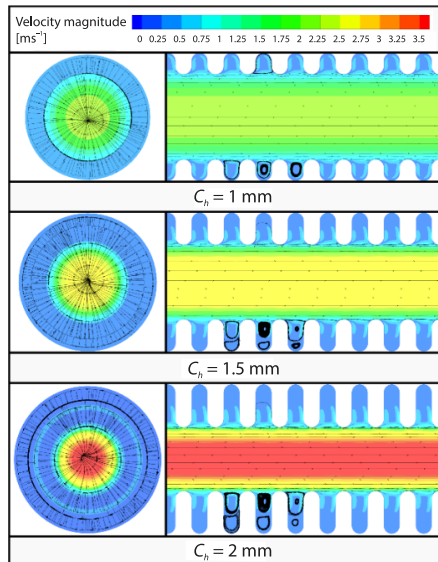


Figure 5. Velocity distributions with different  $C_h$

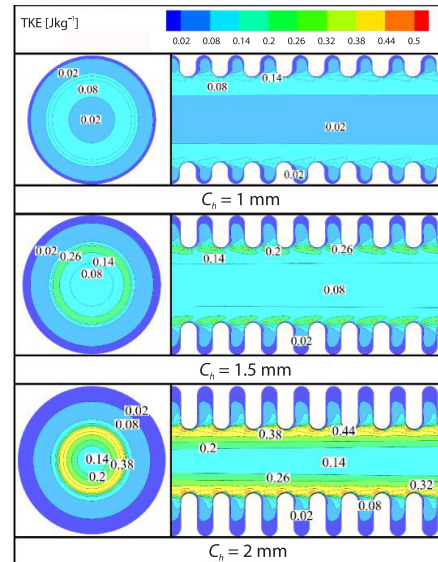


Figure 6. The TKE contour distribution map with different  $C_h$

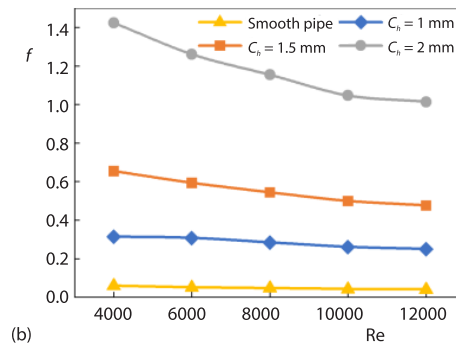
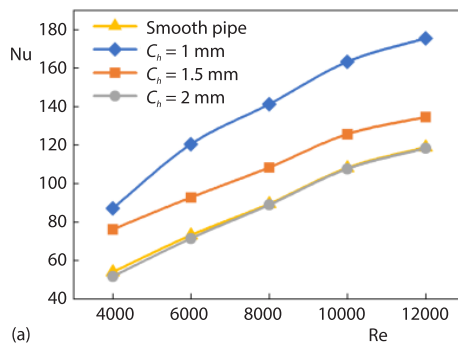


Figure 7. The influence of  $C_h$  on Nusselt number and  $f$ ; (a) Nusselt number and (b)  $f$

number is the same as that of the smooth pipe. When  $C_h$  is 1 mm and 1.5 mm, the difference of Nusselt number between corrugated pipes and smooth pipes is 39.8% and 7.5%, respectively. As  $C_h$  of the corrugated pipe increases, its heat transfer performance is reduced. Therefore, it is necessary to control  $C_h$  within a specific range.

Another critical factor describing convective-enhanced heat transfer is  $f$ , as shown in Figure 7(b). It can be seen that  $f$  has a certain degree of attenuation with the increase of Reynolds number, while  $f$  increases as  $C_h$  increases since the corrugated structure will increase the pressure loss along the pipe-line. All the value of  $f$  under three different  $C_h$  are much higher than those of the smooth pipe, which are 513%, 1074%, and 2361% of the smooth pipe, respectively. It suggests that the increase of secondary flow and vortex at the corrugation leads to more energy dissipation, which increases  $f$ .

The PEF is used to evaluate the thermal performance of the corrugated pipe with different  $C_h$ . When PEF is greater than 1, it indicates that the enhanced heat transfer performance of the corrugated pipe with this structure parameter is better than that of the smooth pipe un-



der certain boundary conditions, not *vice versa* [27]. As shown in fig. 8, when  $C_h$  is 1 mm, 1.5 mm, and 2 mm, PEF are all less than 1, which means that the heat transfer performance of the corrugated structure is not as good as that of the smooth pipe. However, when  $C_h$  is 1 mm and Reynolds number is 4000, PEF is about 0.90. It can be concluded that appropriate reduction of  $C_h$  may increase PEF.

*Effect of corrugation width*

The CFD results of the velocity flow contour with the streamlines field in the pipe-line is shown in fig. 9. It can be seen that when  $C_w$  changes, the velocity distribution does not change much. The reason is that the volume of the main flow region is unchanged, when  $C_w$  changes, its internal velocity distribution is unchanged, while its value is very high. The velocity near the corrugation is low. The vortex will form in the corrugated ring by the fluid-flowing through the corrugated ring striking the corrugated wall. The number of vortexes in the ring decreases as  $C_w$  increases. The vortexes close to the main flow area will stick to the wall due to the liquid-flow in the main flow area. When  $C_w$  is 1 mm and 1.5 mm, new vortexes will form on the outer side of the ring near the outer wall due to the TKE. The formation of these vortexes mainly relies on the energy provided by the central vortex close to the main flow area. Moreover, it will produce a particular wall-cleaning effect.

The contour map distribution of TKE inside the corrugated pipes with three different  $C_w$  is shown in fig. 10. It can be seen that the distribution of TKE with different  $C_w$  is consistent during axial flow, the value near the corrugated ring is high, while the value on the right side of

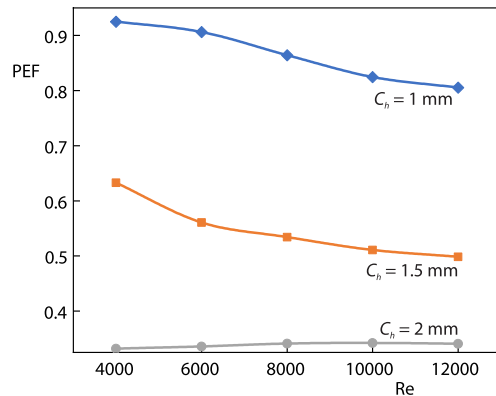


Figure 8. The value of PEF with different  $C_h$

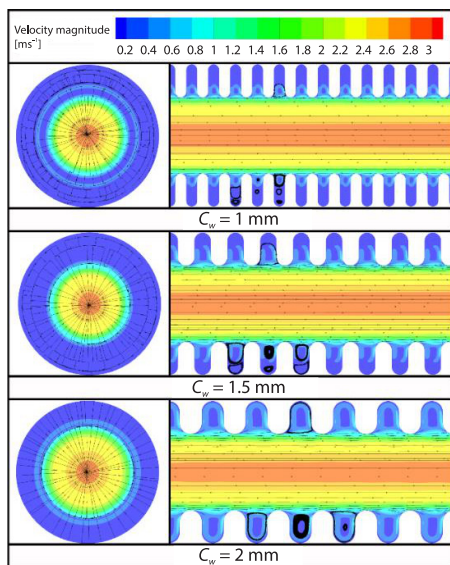


Figure 9. Velocity distribution in pipe with different  $C_w$

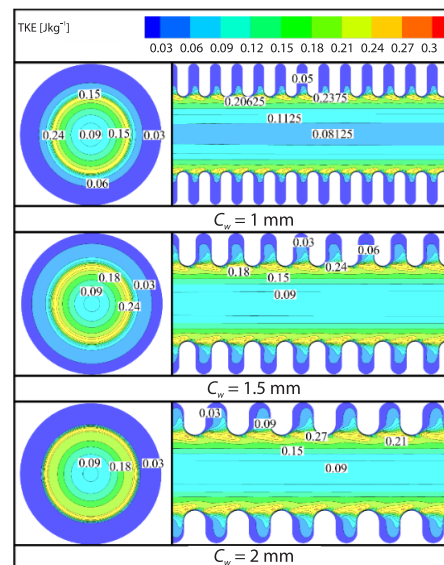


Figure 10. The TKE contour distribution with different  $C_w$

the corrugated ring is higher than that on the left side which is caused by liquid striking the wall. Where TKE is high in the pipe, it is easier to form vortices and flow circulation, destroying the thermal boundary-layer to improve the heat transfer performance. With the increase of  $C_w$ , the TKE value also increases, and the maximum value of TKE is about 0.27 J/kg when  $C_w$  is 2 mm.

Figure 11(a) compares the local Nusselt and Reynolds numbers for smooth and corrugated pipes with different  $C_w$ . It can be seen that Nusselt number increases as Reynolds number increases. When  $C_w$  is 2 mm, it has a higher Nusselt number. As  $C_w$  increases, Nusselt number also increases. Nusselt number of corrugated pipes is higher than that of smooth pipes, where Nusselt number of corrugated pipes with  $C_w$  of 1.5 mm and 2 mm are 7.5% and 40.6% higher than that of smooth pipes, respectively. However, when  $C_w$  is 1 mm, Nusselt number is lower than that of the smooth pipe. It shows that its heat transfer performance could be better than a smooth pipe at a given Reynolds number. Increasing  $C_w$  will improve the heat transfer performance.

It can be seen from fig. 11(b) that the value of  $f$  changes with Reynolds number and generally presents a downward trend for both corrugated pipes with different  $C_w$  and smooth pipes. In addition, it can be noticed that the value  $f$  of the corrugated pipes with different  $C_w$  are all higher than that of smooth pipes. When  $C_w$  increases,  $f$  also increases. However, the difference between the corrugated pipes with different  $C_w$  is 1028.7%, 1075.7%, and 1089.8% compared with the smooth pipes. Generally, the increase in  $C_w$  has little effect on  $f$ .

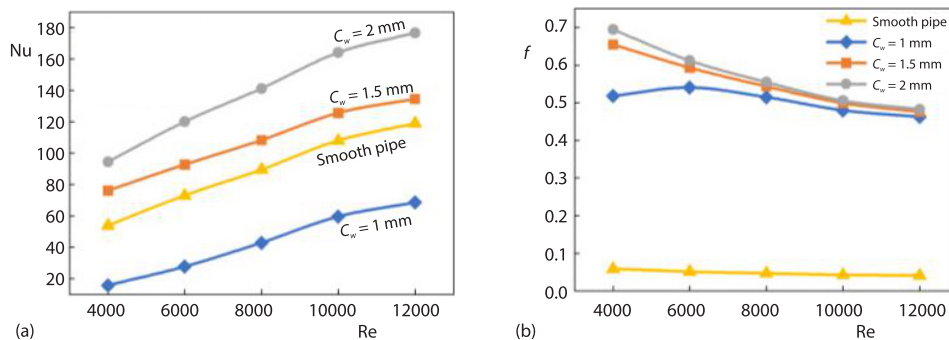


Figure 11. The influence of  $C_w$  on Nusselt number and  $f$ ; (a) Nusselt number and (b)  $f$

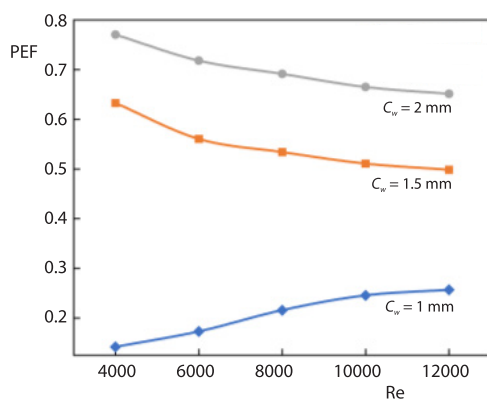


Figure 12. The PEF distribution with different  $C_w$

Figure 12 illustrates the PEF of corrugated pipes with different  $C_w$  to evaluate the improvement of their thermal performance. The results show that  $C_w$  have a significant impact on the heat transfer performance. The PEF becomes larger as  $C_w$  increases, especially when Reynolds number is 4000, where the highest value reaches 0.77. In this case, the damage to the thermal boundary-layer of the corrugated pipes will be more severe. Therefore, when  $C_h$  is fixed, appropriately increasing  $C_w$  can improve PEF.

For the cooling corrugated pipes used in Synchronous Radiation Facility, it should be selected with a higher  $C_h$  and a smaller  $C_w$ . Since the PEF is less than 1, the friction loss increases



in the pipe while the heat transfer coefficient decreases, which can avoid phase change of the coolant due to thermal load. For the heat transfer pipe-line of the monocrystalline silicon cooling system, a corrugated pipe with a  $C_h$  less than 1 mm and a  $C_w$  more than 2 mm is suggested. Because the PEF is greater than 1, its heat transfer performance is better than that of the smooth pipe, which can effectively improve the cooling efficiency.

*Development of correlation equations for Nusselt number and friction coefficient*

In order to study the influence of Reynolds number,  $C_h$ , and  $C_w$  on the heat transfer performance of corrugated pipes, the results of CFD numerical simulation were analyzed by the multiple non-linear regression, and the correlation equations for Nusselt number and  $f$  are established:

$$Nu = 1.0951(Re)^{0.6296} \left(\frac{C_h}{D_h}\right)^{-0.73533} \left(\frac{C_w}{D_h}\right)^{1.333} \tag{6}$$

$$f = 1258.0649(Re)^{-0.29139} \left(\frac{C_h}{D_h}\right)^{2.4956} \left(\frac{C_w}{D_h}\right)^{0.19969} \tag{7}$$

The valid range of this relationship is within Reynolds number (4000-12000), corrugation height ( $C_h = 1-2$  mm), and corrugation width ( $C_w = 1-2$  mm). Moreover, the accuracy of the correlation coefficient,  $R^2$ , is above 94% and 95%. Figures 13 and 14 show the errors of Nusselt number and  $f$ , which are  $\pm 12.4\%$  and  $\pm 13.3\%$  compared with CFD results, respectively.

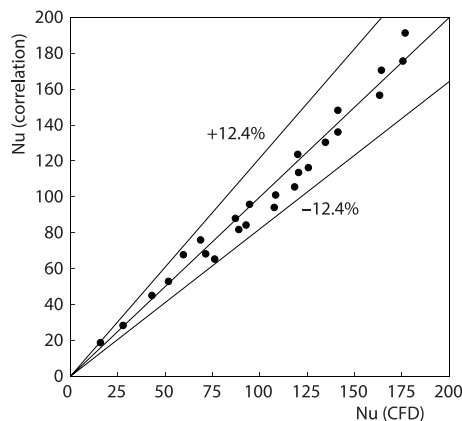


**Figure 13. Comparison of CFD value and predicted Nusselt number**

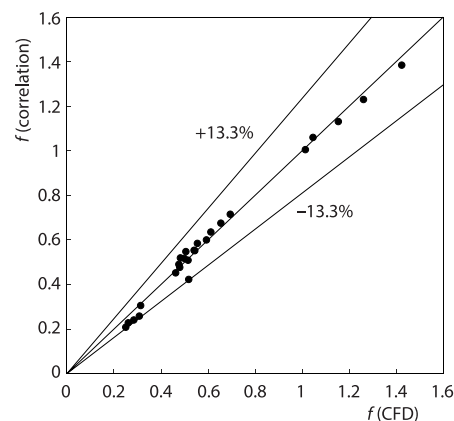


**Figure 14. Comparison of CFD value and predicted  $f$**

**Conclusions**

- Increasing  $C_h$  and  $C_w$  will increase TKE. The main reason is that the liquid-flow strikes the wall of the corrugated pipes to form a large vortex, which increases TKE at the bottom connection of the corrugated ring and destroys the thermal boundary-layer.
- Nusselt number decreases with the increase of  $C_h$ . When  $C_h$  is 2 mm, Nusselt number is smaller than that of the smooth pipe, and when  $C_h$  is 1 mm and 1.5 mm, Nusselt number is more significant than that of the smooth pipe, with a difference of about 39.8 % and 7.5%. Therefore,  $C_h$  can be appropriately reduced to improve the heat transfer performance.

- Increasing  $C_w$  has little effect on  $f$ . When  $C_w$  is 1 mm, its heat transfer performance is not as good as that of a smooth pipe, and when  $C_w$  is 1.5 mm and 2 mm, Nusselt number is larger than that of the smooth pipes, the differences are 7.5% and 40.6%, respectively. Therefore,  $C_w$  can be appropriately enlarged to improve the heat transfer performance.
- When  $C_h$  is 1 mm, 1.5 mm, and  $C_w$  is 1.5 mm, 2 mm, the PEF decreases with the increase of Reynolds number. It is found that in the low Reynolds number range, when  $C_h$  is 1 mm, PEF is 0.90. When  $C_w$  is 2 mm, PEF is 0.77. The accuracy of the equations related to Nusselt number and  $f$  reaches to 94% and 95%.

### Acknowledgment

The authors appreciate greatly the financial support from the Open Fund of State Key Laboratory of Applied Optics, China (No. SKLAO2020001A09), and the Key Research and Development Plan of Shaanxi Province, China (No. 2023-YBGY-346).

### References

- [1] Fu, S., Jiang, G., Potential Application of SSRF in Radiation Oncology: The Aspects of Radiobiology, *Nuclear Science and Techniques*, 20 (2009), 6, pp. 325-330
- [2] Nakanishi, S., *et al.*, Application of Synchrotron Radiation Ultrafast Spectroscopy, *Journal of Synchrotron Radiation*, 5 (1998), 3, pp. 1072-1074
- [3] Leitao, R. G., *et al.*, Elemental Distribution of Prostate Samples by Synchrotron Radiation X-Ray Fluorescence Techniques, *IEEE Transactions on Nuclear Science*, 60 (2012), 2, pp. 722-727
- [4] Tokgoz, N., B. Sahin., Experimental Studies of Flow Characteristics in Corrugated Ducts, *International Communications in Heat and Mass Transfer*, 104 (2019), May, pp. 41-50
- [5] Kurtulmus, N., Sahin, B., A Review of Hydrodynamics and Heat Transfer through Corrugated Channels, *International Communications in Heat and Mass Transfer*, 108 (2019), 104307
- [6] Laohalertdecha, S., Somchai W., The Effects of Corrugation Pitch on the Condensation Heat Transfer Coefficient and Pressure Drop Of R-134a Inside Horizontal Corrugated Tube, *International Journal of Heat and Mass Transfer*, 53 (2010), 13-14, pp. 2924-2931
- [7] Ma, T., *et al.*, Study on Local Thermal-Hydraulic Performance and Optimization of Zigzag-Type Printed Circuit Heat Exchanger at High Temperature, *Energy Conversion and Management*, 104 (2015), Nov., pp. 55-66
- [8] Kwon, H. G., Hwang, S. D., *et al.*, Flow and Heat/Mass Transfer in A Wavy Duct with Various Corrugation Angles in 2-D flow Regimes, *Heat and Mass Transfer*, 45 (2008), July, pp. 157-165
- [9] Jiang, J., *et al.*, Numerical Simulation and Analysis of Enhanced Heat Transfer in Corrugated Tube Heat Exchanger, *IOP Conference Series: Earth and Environmental Science*, IOP Publishing, 467 (2020), 1
- [10] Jaffal, H. M., *et al.*, The Effect of Interruptions on Thermal Characteristics of Corrugated Tube, *Case Studies in Thermal Engineering*, 25 (2021), 100910
- [11] Al-Obaidi A. R., Alhamid J., Investigation of Flow Pattern, Thermohydraulic Performance And Heat Transfer Improvement in 3-D Corrugated Circular Pipe under Varying Structure Configuration Parameters with Development Different Correlations, *International Communications in Heat and Mass Transfer*, 126 (2021), 105394
- [12] Al-Obaidi A. R., Investigation on Effects of Varying Geometrical Configurations on Thermal-Hydraulics Flow in a 3-D Corrugated Pipe, *International Journal of Thermal Sciences*, 171 (2022), 107237
- [13] Al-Obaidi A. R., Alhamid J., Investigation of the Effect of Various Corrugated Pipe Configurations on Thermo-Hydraulic Flow and Enhancement of Heat Transfer Performance with the Development of Different Correlations, *International Journal of Thermal Sciences*, 176 (2022), 107528
- [14] Han, H.-Z., *et al.*, Numerical Study of Flow and Heat Transfer Characteristics in Outward Convex Corrugated Tubes, *International Journal of Heat and Mass Transfer*, 55 (2012), 25-26, pp. 7782-7802
- [15] Ajeel, R. K., *et al.*, Turbulent Convective Heat Transfer of Silica Oxide Nanofluid through Corrugated Channels: An Experimental and Numerical Study, *International Journal of Heat and Mass Transfer*, 145 (2019), 118806
- [16] Mohammed, H. A., *et al.*, Influence of Geometrical Parameters and Forced Convective Heat Transfer In Transversely Corrugated Circular Tubes, *International Communications in Heat and Mass Transfer*, 44 (2013), May, pp. 116-126

- [17] Dong, Y., *et al.*, Pressure Drop, Heat Transfer and Performance of Single-Phase Turbulent Flow in Spirally Corrugated Tubes, *Experimental Thermal and Fluid Science*, 24 (2001), 3-4, pp. 131-138
- [18] Vicente P. G., *et al.*, Experimental Investigation on Heat Transfer and Frictional Characteristics of Spirally Corrugated Tubes in Turbulent Flow at Different Prandtl Numbers, *International Journal of Heat and Mass Transfer*, 47 (2004), 4, pp. 671-681
- [19] Pethkool, S., *et al.*, Turbulent Heat Transfer Enhancement in a Heat Exchanger Using Helically Corrugated Tube, *International Communications in Heat and Mass Transfer*, 38 (2011), 3, pp. 340-347
- [20] Corcoles, J. I., *et al.*, Numerical and Experimental Study of the Heat Transfer Process in a Double Pipe Heat Exchanger with Inner Corrugated Tubes, *International Journal of Thermal Sciences*, 158 (2020), 106526
- [21] Ahmed, M. A., *et al.*, Numerical Investigations of Flow and Heat Transfer Enhancement in a Corrugated Channel Using Nanofluid, *International Communications in Heat and Mass Transfer*, 38 (2011), 10, pp. 1368-1375
- [22] Qi, C., *et al.*, Experimental and Numerical Research on the Flow and Heat Transfer Characteristics of TiO<sub>2</sub>-Water Nanofluids in a Corrugated Tube, *International Journal of Heat and Mass Transfer*, 115 (2017), Part B, pp. 1072-1084
- [23] Hatami, M., *et al.*, Numerical Heat Transfer Enhancement Using Different Nanofluids Flow through Venturi and Wavy Tubes, *Case Studies in Thermal Engineering*, 13 (2019), 100368
- [24] Wan, Y., *et al.*, Experimental Study on Thermo-Hydraulic Performances of Nanofluids Flowing through a Corrugated Tube Filled with Copper Foam in Heat Exchange Systems, *Chinese Journal of Chemical Engineering*, 26 (2018), 12, pp. 2431-2440
- [25] Naphon, P., Songkran W., Pulsating Flow and Magnetic Field Effects on the Convective Heat Transfer of TiO<sub>2</sub>-Water Nanofluids in Helically Corrugated Tube, *International Journal of Heat and Mass Transfer*, 125 (2018), Oct., pp. 1054-1060
- [26] Wu J, *et al.*, Improvement of the Performance of a Cryo-Cooled Monochromator at SSRF – Part II: Angular Stability of the Exit Beam, *Nuclear Instruments and Methods in Physics Research Section A, Accelerators, Spectrometers, Detectors and Associated Equipment*, 988 (2021), 164872
- [27] Omid, M., *et al.*, Numerical Study on the Effect of Using Spiral Tube with Lobed Cross-Section in Double-Pipe Heat Exchangers, *Journal of Thermal Analysis and Calorimetry*, 134 (2018), 3, pp. 2397-2408